斜齿圆柱齿轮瞬时啮合刚度及齿廓修形的研究*

常山　徐振忠　霍肇波　　陈谌闻　　孟祥生
(哈尔滨七〇三研究所)　(哈尔滨工业大学)　(清华大学)

[摘要]本文提出了一种高效的考虑齿轮基体影响的齿轮计算模型,根据有限元柔度矩阵法,编制了一套刚度计算程序,给出了斜齿轮啮合过程中瞬时啮合刚度变化率与轴向重合度之间的关系。在刚度计算基础上,利用内点罚函数法的优化思想编制了一套修形计算程序,对斜齿轮的齿廓修形进行了深入研究。

关键词　瞬时啮合刚度　齿廓修形　柔度矩阵　内点罚函数
分类号　TH132.41

0　引言

轮齿变形与刚度随啮合位置变化规律的研究是轮齿修形、动态特性、故障诊断以及寿命预测等研究的基础。选择合理的有限元模型是准确求解该问题的前提,本文在反映斜齿轮真实结构的基础上提出了一种包括轮体的有限元模型。关于轮齿修形问题国内外学者做了许多积极尝试[1-5],文献[1-2]中提出的线性规划法具有一定的代表性,但线性规划法在进行多目标优化修形时很难处理,本文成功地将内点罚函数法引入到修形研究中,得到了更为满意的结果。

1　瞬时啮合刚度的计算

如图 1所示,受载齿轮副在啮合过程中从动齿轮相对主动齿轮有一回转滞后量,反映到啮合线上即是齿轮副的啮合变形 $W(r)$,本文定义在任意啮合位置的瞬时啮合刚度为:

$$C(V_i)=\frac{W_n}{W(r_i)}=\frac{T_1}{r_{b1}\cdot b\cdot W(r_i)} \qquad (1)$$

式中: W_n—— 单位齿宽端面法向载荷 (N/mm);
T_1—— 主动齿轮的传递扭矩 (N·mm);
r_{b1}—— 主动齿轮基圆半径 (mm);
b—— 齿宽 (mm)。

由式(1)可见,求解任意啮合位置的瞬时啮合刚度的实质是求解该位置的啮合变形,本文采用三维有限元柔度矩阵法来求解。

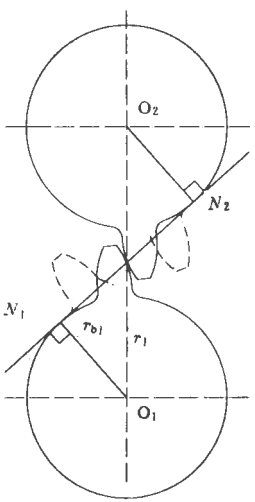

图 1　轮齿啮合变形

将同时啮合的几条接触线离散为若干微段,各微段所承担的线载荷转化为集中载荷作用在微段的中点上,利用有限元法求出各节点的柔度,再结合变形协调条件和力平衡条件可建立起以节点力和啮合变形为未知量的线性方程组。求解此方程组便可求得啮合变形及接触线上的载荷分布。所谓变形协调

* 博士点基金资助课题
收稿日期　1996-03-25　修改定稿　1997-06-13

条件是指同时啮合的几条接触线上的节点具有相同的啮合变形,即有 $W_1 = W_2 = \cdots = W_n = W$。但由于系统变形和各种误差的影响,相啮合轮齿沿接触线接触时满足 $W + e_1 = W + e_2 = \cdots = W + e_n = W$,而力平衡条件是指接触线上各节点作用力的切向分量与主动轮基圆半径乘积之和等于主动轮上所担负的扭矩,即有

$$\sum_{i=1}^{n} \cos\beta_b \cdot r_{b1} \cdot P_i = T_1 \qquad (2)$$

引入柔度系数,写成方程组的形式

$$\begin{aligned}
&\lambda_{11}P_1 + \lambda_{12}P_2 + \cdots + \lambda_{1n}P_n - W = -e_1\\
&\lambda_{i1}P_1 + \lambda_{i2}P_2 + \cdots + \lambda_{in}P_n - W = -e_i\\
&\lambda_{n1}P_1 + \lambda_{n2}P_2 + \cdots + \lambda_{nn}P_n - W = -e_n\\
&P_1 + P_2 + \cdots + P_n = T_1/(r_{b1}\cdot\cos\beta_b)
\end{aligned}$$

式中: P_i—— 节点 i 的作用载荷 (N);

λ_{ij}—— 节点 j 处作用单位力引起的主、被动轮齿在 i 点的法向变形之和;

e_i—— 节点 i 处的综合误差;

β_b—— 齿轮基圆螺旋角。

2 有限元模型的确定及网格的自动划分

有限元柔度矩阵法的实质是求出同时啮合的几对轮齿接触线上节点的柔度,只要根据每条接触线在齿面上的具体位置,调整模型齿面节点坐标,用一对齿便可算出所有接触节点的柔度,因此建立模型

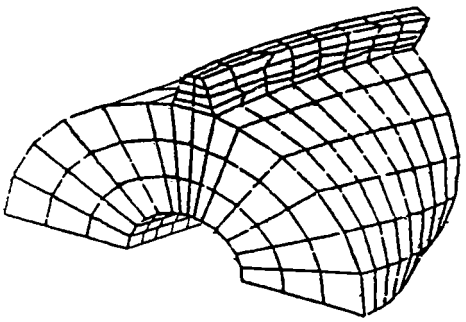

图 2　三维有限元计算模型

时只需考虑一对齿即可。根据 Tulpin[3]的分析,在计算瞬时啮合刚度时应考虑轮体的周向变形。为此本文编制了包含整个轮体的计算模型,经过计算比较最后确定计算模型如图 2所示。有限元网格由程序自动生成,无需人工干预,计算时只输入齿轮副的基本参数和齿轮啮合位置参数即可生成所要求的三维有限元数据文件。

3 齿轮啮合刚度计算结果及分析

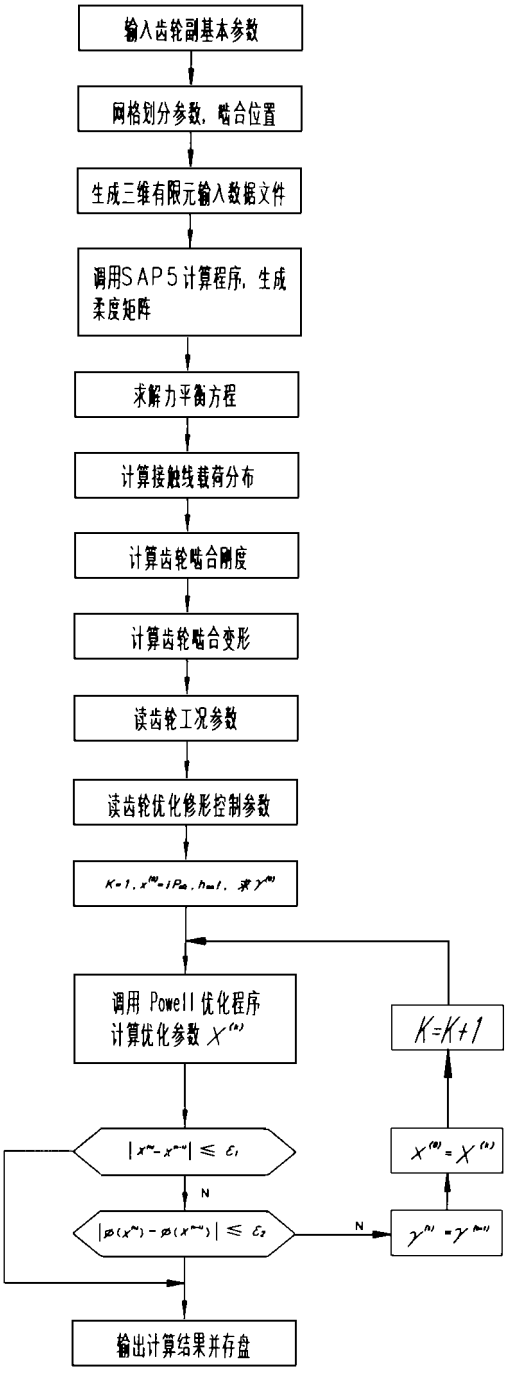

图 3　齿轮啮合刚度和优化修形计算程序流程图

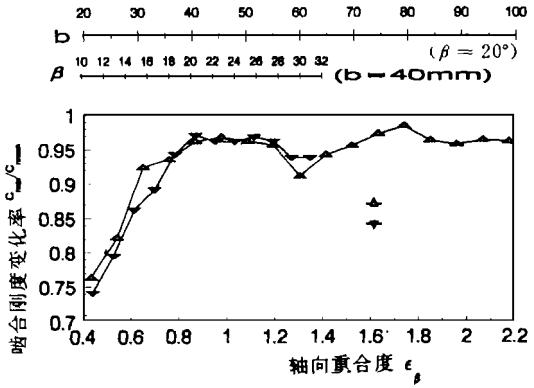

图 4 刚度变化率与轴向重合度

3.1 直齿轮单对齿啮合刚度

根据上述理论和方法,作者编制了一套齿轮瞬时啮合刚度和优化修形的计算程度,程序流程图如图 3所示。所用该程序计算了一对直齿轮的啮合刚度,所取齿轮副参数如下 Z_1= Z_2= 25, m_n= 5 mm, α_n = 20°, x_1= x_2= 0, b= 40 mm, h_0^* = 1.0, C^* = 0.5,齿轮不进行任何修形。三维有限元柔度矩阵法计算齿轮啮合刚度结果为 C = 15.45N/(mm·μm),利用国际 GB3480所给出的计算公式得到的啮合刚度 C = 15.68 N/(mm·μm),相差 1.8%,由此可以看出,本文所采用的计算模型是合理的。

3.2 斜齿轮瞬时啮合刚度

利用齿轮啮合刚度计算程序,考察齿轮瞬时啮合刚度变化率(一个啮合周期中最小刚度与平均刚度的比值)与轴向重合度之间的关系。除齿宽 b 和螺旋角 U外,其他齿轮参数与 3.1节相同。计算结果如图 4所示,图中曲线 1对应于齿宽 b= 40mm,螺旋角 β从 12°~ 32°等间隔变化,曲线 2对应于螺旋角 U= 20°,齿宽从 20 mm~ 100 mm等间隔变化。曲线 1与曲线 2的变化规律很相似,这说明:刚度变化率与轴向重合度有着直接关系,因此在齿轮设计中可以通过合理选择齿宽和螺旋角来降低瞬时啮合刚度的波动幅度。

4 斜齿轮齿廓修形

载荷分布与啮合刚度是修形形貌的直接函数,通过选择合适的修形参数,可以得到有利的载荷分布及较低的激振[2]。作者编制了一套齿轮齿廓修形优化程序,从减少冲击、改善载荷分配与分布、降低啮合过程中瞬时啮合刚度波动幅度等几方面来确定最佳的修形参数(修形量、修形高度、修形曲线)。

4.1 综合目标函数

$$\mathrm{H}(\vec{x}) = w_1 f_1(\vec{x}) + w_2 f_2(\vec{x}) - \mathrm{V}^{(K)} \sum g_i(\vec{x}) \tag{4}$$

式中: $\vec{x}$修形参数向量, $\vec{x}$= (P_m, h_m);

$\mathrm{V}^{(K)}$—— 惩罚因子;

$w_{1,2}$—— 加权因子;

$f_1(\vec{x})$—— 载荷或应力目标函数;

$f_2(\vec{x})$—— 刚度目标函数;

$g_i(\vec{x})$—— 惩罚函数项。

4.1.1 应力目标函数

本文的参数寻优是从提高轮齿接触疲劳强度的角度来考虑的,亦即修形参数的选择应使得整个啮合过程中同时参与啮合的各轮齿的齿面接触应力分布趋于相同。用函数形式可描述如下:

$$f_1(\vec{x}) = \sqrt{\sum_{i=1}^{m}\sum_{j=1}^{n} [e_j(\vec{x}) - \frac{1}{n}\sum e_j(\vec{x})]^2} \tag{5}$$

式中: m—— 啮合位置数;

n—— 接触线上的节点数;

$e_j(x)$—— 接触点的接触应力。

预先选定啮合周期内的 m 个啮合位置,利用程序计算出各个啮合位置的柔度矩阵。对应于每个啮合位置,根据修形曲线与修形参数确定各条接触线上节点处的修形量,作为误差向量,进而求解方程组(3),得出各个啮合位置的载荷分布与啮合变形,而后按相应公式求出应力值,然后计算各个啮合位置的应力均方和,最后计算整个啮合过程的应力均方根。

4.1.2 刚度目标函数

啮合过程瞬时啮合刚度的变化是引起齿轮副振动的一个主要原因,为了减小动载荷和噪声,修形参数的选取应使得啮合过程中瞬时啮合刚度的变化幅度最小,用函数形式可描述如下:

$$f_2(\vec{x}) = \sqrt{\sum_{i=1}^{m} [C_i(\vec{x}) - \frac{1}{m}\sum_{i=1}^{m} C_i(\vec{x})]^2} \tag{6}$$

式中: $C_i(\vec{x})$—— 任意啮合位置的瞬时啮合刚度。

4.1.3 惩罚函数

惩罚函数是用来描述修形参数的取值范围

$$\begin{cases} g_1(\vec{x}) = P_m - P_{m0} \leqslant 0 \\ g_2(\vec{x}) = h_m - h_{m0} \leqslant 0 \end{cases} \quad (7)$$

P_{m0},h_{m0}分别为最大修形量与最大修形高度,P_{m0}的确定是以使啮入或啮出点的载荷为零为前提的,h_{m0}可以取为 2/3齿全高。

4.2 接触点的修形量计算

本文采用两种修形曲线,一种为直线修形,另一种为半立方抛物线修形。修形方式采用主从动齿轮的齿顶修形,齿根和齿向都不修形。

a.直线修形

$$\begin{cases} m_p = P_m \cdot \dfrac{r_p - (r_a - h_m)}{h_m}, r_p > r_a - h_m \\ m_p = 0 \quad r_p \leqslant r_a - h_m \end{cases} \quad (8)$$

b.半立方抛物线修形

$$\begin{cases} m_p = P_m \cdot \left[\dfrac{r_p - (r_a - h_m)}{h_m}\right]^{3/2}, r_p > r_a - h_m \\ m_p = 0 \quad r_p \leqslant r_a - h_m \end{cases} \quad (9)$$

在式(8)和式(9)中,m_p为接触点修形量,r_p为接触点向量半径,h_m齿顶修形长度,r_a为齿顶圆半径。

4.3 齿轮齿廓修形计算结果与分析

计算齿轮副参数为: $Z_1 = Z_2 = 25$, $m_n = 5$ mm, $\alpha_n = 20°$, $U = 18°$, $x_1 = x_2 = 0$, $b = 40$ mm。主动齿轮扭矩 $T = 890$ N·m,计算结果如图 5所示。图 5(a)中曲线,为修形前后齿轮副一个啮合周期内的轮齿刚度变化规律,曲线 2、3分别为直线修形和半立方抛物线修形后的结果。其中,直线修形的最优参数为 $P_m = 20\mu$m, $h_m = 3.75$ mm,半立方抛物线修形的最优参数为 $P_m = 25\mu$m, $h_m = 4$ mm。图 5(b)中曲线 1,2和 3分别为修形前、直线修形和抛物线修形时齿轮副一个啮合周期内齿面接触应力梯度的变化规律,曲线上的每一点对应于某一啮合时刻同时啮合的几对齿中最大齿面接触应力与平均值的比值。齿面接触应力采用文献[5]中所述的方法计算。由图 5可以看出,只要合理选择最佳修形量、修形长度、修形曲线就可以同时取得降低啮合过程中轮齿刚度波动幅度和改善接触线载荷分布的双重效果。

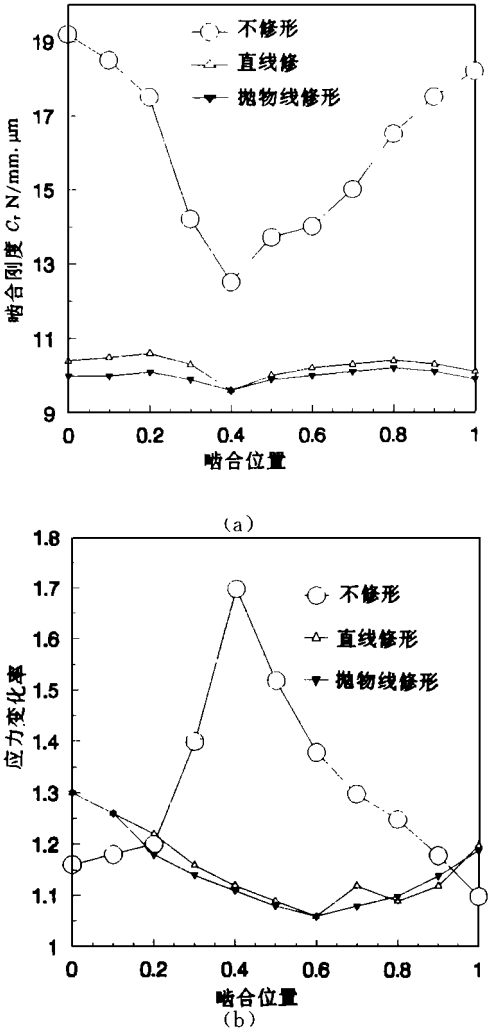

图 5 齿轮优化修形的计算结果

5 结论

(1)本文提出了一种高效合理的斜齿轮有限元计算模型,在此基础上对斜齿轮的轮齿刚度问题进行了深入研究。计算结果表明:轴向重合度是决定齿轮瞬时啮合刚度变化的重要因素,设计时应合理选择螺旋角和齿宽以使瞬时啮合刚度波动尽可能小,达到减振降噪的目的。

(2)为深入研究齿轮修形将内点罚函数法引入修形研究中,开辟了齿轮修形研究的新思路。利用该方法有效地解决了多目标修形优化设计问题,计算结果表明,只要合理选择齿轮修形参数可以同时取

得降低啮合过程中轮齿刚度波动幅度和改善接触应力分布的双重效果。

参 考 文 献

1 方宗德,沈允文.斜齿轮三维修形的优化设计.机械工程学报,1992,(6):57-61

2 Weck M. Optimum tooth flank corrections for helical gears. Proc 1989 Int Power Transm Gearing Conf.

3 Tuplin W A. Gear Load Capacity. Sir Isacc Pitman & Sans. Ltd., 1962

4 Simon V. Load and stress distributions in spur and helical gears. ASME Journal of Mechanisms Transmissions, and Automations in Design, 1988, 110: 197-202

5 Schmidt G R. Optimum tooth profile correction of helical gears. Third international Power Transmission and Gearing Conference, San Francisco, 1980: DET-110

(渠源 编辑)

作者简介 常 山,男,1965年6月生,中国舰船研究院博士后.在哈工大学报(英文版)等杂志上发表科技论文二十余篇。主要从事齿轮动力学、齿轮修形技术等方面的研究。(通讯地址 150036哈尔滨 77-5信箱)

新技术

级联增湿涡轮电站设计

据“Gas Turbine World”1996年5-6月号报道,级联先进涡轮“CAT)和级联增湿涡轮(CHAT)电站设计已稳定地进展。

基本设计使用空气作为工作流体,它在二个单独轴-动力生产轴和平衡轴之间运动或“级联”,运动的空气按需要在压缩和膨胀循环中间被加热和冷却。

CHAT装置过程开始于通过空气过滤器抽取的环境空气进入动力产生轴上的低压轴流压气机。低压压气机排出的空气流指向第二根轴上的一段中压压气机的第一个轴流段。中压压气机第一段的排气通往水冷的中间冷却器,然后到第二根轴上的中压压气机的第二个离心段。中压压气机第二段的排气通到第二个中间冷却器,然后进入高压压气机入口。在其进入饱和器中被增湿和预热(使用中间冷却器和排气余热回收加热器中产生的热水)之前,空气在筒式高压压气机内被压缩到系统的最大压力。从饱和器出来,空气通到回热器进一步预热,然后通到高压燃烧室/涡轮组件。燃料被加入高压燃烧室。在供入低压燃烧室/涡轮前,热燃气在高压涡轮中膨胀。低压燃烧室使燃气流温度增加到其设计值(1349℃),然后燃气通过501F的涡轮膨胀作功。涡轮排气通过回热器和水加热段,然后排入烟囱。

研究表明,级联增湿涡轮电站具有效率高(54.7%)、投资费用低(350-400美元/kW)、部分负荷性能好、NO_x排放低(低于10ppm)等优点。

(思娟 供稿)

chanical Industry. **Key words**: surge, anti-surge control system

太阳能吸附式空气取水器和太阳能制冷结露法空气取水器的热性能分析比较= **An Analytical Comparison of Thermodynamic Performance of Solar-energy Adsorption-based Water Collector from Air and Solar Energy Refrigeration Dewfall-based Water collector from Air**[刊,中]/Chou Qiaoli, Liu Zongyan, et al. (China National University of Science & Technology) //Journal of Engineering for Thermal Energy & Power. - 1997, 12(4). - 253~256

A thermodynamic performance is conducted of an adsorption type water collector from air and a refrigeration dewfall based water collector from air with a water collection expression being given. On the basis of the said expression a comparison has been made of the water collection rate of the above-cited two methods. **Key words**: water collector from air, adsorption refrigeration, refrigeration dewfall method, water collection rate

泥炭燃烧的研究= **A Study on Peat Combustion**[刊,中]/Zhang Jingbo, Li Xueheng et al (Northeast Electrical Engineering Institute) //Journal of Engineering for Thermal Energy & Power. - 1997, 12(4). - 257~260

On the basis of peat basic combustion tests and the development and operation practice of a 1 t/h peat-fired fluidized boiler this paper proposes a method of firing peat by utilizing fluidized bed combustion technology. A detailed description is given of the peat combustion characteristics with some key issues in the design of such boilers being pinpointed. **Key words**: boiler, fluidized bed, peat, combustion

煤粉粒子的发射率= **The Emissivity of Pulverized-Coal Particles**[刊,中]/Liu Linhua, Yu Qizheng, Tan Heping (Harbin Institute of Technology), Xu Wanli (Harbin University of Science & Technology) //Journal of Engineering for Thermal Energy & Power. - 1997, 12(4). - 261~266

On the basis of the classical Lorentz-Mie electromagnetic theory for isotropic and homogeneous spherical particles and by utilizing the experimentally measured complex refractive indices of pulverized-coal particles determined are the emissivity of pulverized-coal particles of twenty kinds of Chinese coals for power generation. The results of calculation show that the full wave-length emissivity of pulverized-coal particles is dependent on particle diameter, particle temperature and coal type and within a wide range of particle diameters radically deviates from the assumed value of 0.8 often given in technical literature. It has also been found that within a particle diameter range of 1~20 μm the emissivity of the pulverized-coal particles is often greater than 1.0. The reason why some pulverized-coal particles have an emissivity greater than 1.0 is given with an explanation of its physical meaning. For engineering calculation purposes the curves showing the variation of emissivity with particle diameter and temperature are given for twenty kinds of typical Chinese coals. **Key words**: emissivity, particles, coal, electromagnetic theory

一类不可逆卡诺热机最佳效率和功率间的关系= **Relationship between the Optimum Efficiency and Output Power of a Kind of Irreversible Carnot Heat Engine**[刊,中]/Lu Ying, Tian Xinquan (Luoyang Teachers College) //Journal of Engineering for Thermal Energy & Power. - 1997, 12(4). - 267~269

Through the use of an irreversible Carnot heat engine model of Dulong-Petit nonlinear heat transfer rate and heat leakage derived is its basic optimization relation with the issue of the heat engine efficiency during its maximum output power being also discussed. **Key words**: finite-time thermodynamics, Carnot engine, thermal resistance, heat leakage, basis optimization ralation, optimum efficiency

斜齿圆柱齿轮瞬时啮合刚度及齿廓修形的研究= **A Study on the Momentary Meshing Rigidity and Tooth Profile Modification of Helical Cylindrical Gears**[刊,中]/Chand Shan, Xu Zhenzhong, Huo Zhaobo (Harbin No. 703 Research Institute) //Journal of Engineering for Thermal Energy & Power. - 1997, 12(4). - 270~274

The paper presents a high-efficiency gear calculation model with gear basic effects being taken into ac-

count. By employing a finite-element flexibility matrix method the authors have drawn up a set of rigidity calculation procedures, providing the relationship between the momentary meshing rigidity variation rate and axial congruence during the axial gear meshing process. On the basis of the rigidity calculation and by utilizing the optimization concept of inner point penalty function method a full set of calculation procedures for gear shape modification was prepared and an in-depth study of the tooth profile modification of helical gears conducted. **Key words**: momentary meshing rigidity, tooth profile modification, flexibility matrix, inner point penalty function

管内在线防垢及强化传热的实验研究= **An Experimental Study of On-line Fouling Prevention Inside Tubes and the Intensification of Heat Transfer**〔刊,中〕/Xiao Hongliang, Zhu Dongsheng, Tan Yingke(South China University of Science & Technology) //Journal of Engineering for Thermal Energy & Power. – 1997, 12(4), – 275~ 277

With saturated $CaCO_3$ serving as a material a study is conducted of the fouling prevention, heat transfer augmentation and structural parameters of a moving spring coil in a heater tube as well as the interrelated effects of operating variables. The paper discusses and presents the experimental study results of anti-fouling and heat transfer intensification mechanism with a theoretical basis for the said results being given, **Key words**: heater, inserted object, scale-formation, intensified heat transfer

碳酸钙分解的试验研究= **An Experimental Study on the Decomposition of Calcium Carbonate**〔刊,中〕/Yu Zhaonan(Zhejiang University) //Journal of Engineering for Thermal Energy & Power. – 1997, 12(4). – 278~ 280

By the use of a high-precision thermobalance an experimental study was performed of the decomposition of small particles of $CaCO_3$, resulting in a clarification of the effect of particle size, heating rate and impurities on the decomposition of $CaCO_3$. The mechanism of the above-cited decomposition was studied with an interpretation given for such phenomena, **Key words**: calcium carbonate, decomposition, test

青山烟煤及其燃后飞灰中有机污染物分布的研究= **An Investigation of the Distribution of Organic Pollutants from Qingshan Bituminous Coal and its Post-combustion Fly Ash**〔刊,中〕/Xu Minghou, Yan Rong, Long Yuxuan, Hao Liang(Huazhong University of Science & Technology) //Journal of Engineering for Thermal Energy & Power, – 1997, 12(4), – 281~ 284

With the help of a GC/MDS system determined from the extractive solutions of 7 hours, 16 hours and 24 hours the sort and content of such a variety of organic pollutants as aliphatic chains, benzene families and polycyclic aromatic hydrocarbons(PAHs), and obtained are the distribution characteristics of the organic pollutants of Qingshan bituminous coal and its fly ash products. The test results show that there are several kinds of organic pollutants, especially PAHs, in the raw coal itself. The different sorts and content of benzene families in the fly ash will increase while those of the PAHs decrease following the combustion of the raw coal. The rational organization of the combustion process can play a significant role in achieving a decrease in organic pollutants. **Key words**: bituminous coal, combustion product, organic pollutants, measurement, distribution characteristics, fly ash

循环流化床气固两相间传热特性的实验研究= **An Experimental Study of Gas/Solid Interphase Heat Transfer Characteristics of a Circulating Fluidized Bed**〔刊,中〕/Zheng Shouzhong, Lu Feng, et al(Southeastern University) //Journal of Engineering for Thermal Energy & Power. –1997, 12(4). –285~ 288

On a small-sized test stand and by using a dual thermocouple temperature measuring method determined is the temperature of a fluidized-bed layer. The test results show that the gas/solid interphase heat transfer mainly takes place in the lower half portion of the circulating bed. The increase in gas apparent flow speed, the